Engineering Structures 245 (2021) 112880

Contents lists available at ScienceDirect

Engineering Structures

journal homepage: www.elsevier.com/locate/engstruct

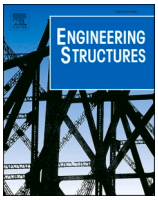

Factors affecting slip and stress distribution of concrete slabs in composite beams

Ahmed Kamar [a], Mahmoud Lasheen [b,*], Amr Shaat [c], Amr Zaher [c], Ayman Khalil [c]

[a] Department of Building and Constructing Engineering, October 6 University, Giza, Egypt
[b] Concrete Construction Research Institute, Housing and Building National Research Center, Cairo, Egypt
[c] Department of Structural Engineering, Ain Shams University, Cairo, Egypt

ARTICLE INFO

Keyword:
Composite beam
Shear connector
Slip
Strain distribution
Reinforcement ratio
Concrete crack
Poisson's ratio

ABSTRACT

An experimental program is carried out to examine the effects of different factors on the slip and stress distribution of concrete slabs in composite beams. A total of ten steel–concrete composite beams with a span of 4.80 m are tested to find the effects of the type of shear connectors and the concrete slab reinforcement on the behaviour of composite beams. All beams consist of monosymmetric steel cross-sections connected to 120 cm wide concrete slabs. Welded shear connectors (angles or channels) spaced at 20 cm are used to connect the concrete slabs to the steel beams. The concrete slabs of eight beams are provided with a lower steel reinforcement only while two beams are provided with both lower and upper steel reinforcement. The results showed that the ultimate load capacity of composite beam with channel connectors is 14% higher than the counterpart beam with angle connectors and 30% stiffer in resisting the slip of the concrete slab. Moreover, composite beams with channel connectors tend to maintain strain compatibility at the interface between concrete slab and steel section better than the counterpart beams with angle connectors. It is also found that using upper steel reinforcement mesh enhances the stress distribution in the concrete slab until failure. It is found that increasing the reinforcement ratio of the concrete slab from 0.18% to 0.46% increases the flexural strength of the composite beams by 7.45%, while decreases the deflection values by 23%. Moreover, using upper steel reinforcement prevented the longitudinal cracking of the top surface of the concrete slab and allowed for full plastification of the steel cross-sections.

1. Introduction

In steel–concrete composite beams, the steel embedment inside the concrete slab such as the shear connectors and reinforcement bars plays important role in the overall behaviour of the beams. The design of shear connectors is crucial in determining the degree of composite action and consequently evaluating the slip of the concrete slab. On the other hand, the reinforcement bars inside the concrete slab can have an impact on the stress and strain redistribution along the transverse direction of the slab as well as reducing the vertical deflection of the beam. In this paper, the effect of shear connectors and steel reinforcement on the behaviour of composite beams is studied.

There are many types of shear connectors such as studs, dowels, angles, and channels [1–4]. The channel sections are considered the most popular type used in composite girders due to their geometric pattern that helps in achieving efficient better anchoring with the concrete slab. The degree of composite action is an important parameter in the design of composite beams due to its influence on their flexural strength and deformations. The degree of composite action depends on the rigidity and number of shear connectors and can simply be defined as the ratio between the total horizontal shear capacity of the connectors in the shear span and the smaller strength of either the steel section or the concrete slab compressive capacity. The reduction in the percentage of composite action results in higher slip values at the interface between the steel beam and the concrete slab, potentially resulting in increased deflection values of the composite beams. The slip rate between the concrete slab and the steel section, which is greatly affected by the type of shear connectors, is very important in understanding the behaviour of the composite beam [5]. The resistance of the shear connectors is also dependent on the relative distance between their center of gravity and the line of action developed by the concrete slab shear force [6]. The failure of connectors depends mainly on the geometry and location of

* Corresponding author.
E-mail address: Lasheen_9000@yahoo.com (M. Lasheen).

https://doi.org/10.1016/j.engstruct.2021.112880
Received 23 February 2021; Received in revised form 4 July 2021; Accepted 17 July 2021
Available online 2 August 2021

the connectors as well as the concrete compressive strength [7]. It was shown that the angle shear connectors achieved higher shear capacity associated with lower ductility [8–10].

The stiffness and strength of composite beams are influenced by the type of shear connectors and the provided degree of composite action. The strain profile along the composite beam depth does not solely depend on the degree of shear connection but also on the connector type [11–15]. Moreover, the more ductile shear connectors at the steel–concrete interface may cause force redistribution along the cross-section, which enhances the overall ductility of the composite beam [16].

Due to the non-uniform compressive stress distribution along the concrete slab of composite beams, designers adopt the concept of effective slab width to simplify the calculations of the flexure capacity and deflection of such beams. The non-uniform longitudinal stress distribution along the width of the concrete slab; namely the shear lag; usually takes high values over the connected steel beam while the stresses decrease at the extremities [17-19].

The accurate estimate of the effective concrete slab width in composite beams leads to an accurate prediction of both strength and deflections. The calculation of the effective slab width in most of the international codes depends on the span of the composite beam and the spacing between beams. The effective width relies on the loading level. Where, the effective concrete slab width increases with increasing the load beyond the elastic phase and reaches the complete slab width near the collapse [16,20]. Recent research studies indicated that both the size of the steel section, represented by its radius of gyration, and percentage of composite action have noticeable effects on the values of the effective width, and hence the stiffness and strength of composite beams [16,20]. Comprehensive literature review for many international codes (i.e., AISC 360–15 [21], CISC S16-14 [22] and the Eurocode 4; CEN 2004 [23]) indicated that providing sufficient reinforcement in the transverse direction resists the tensile stresses in the concrete slab and prevents the longitudinal cracks. However, the strength equations of steel–concrete composite beams do not account for the contribution of the transverse reinforcement. It is expected, however, that transverse reinforcement has a contribution in delaying or completely preventing the initiation of longitudinal cracks in the concrete slab with a potential increase in the flexural capacity of composite beams [24]. Therefore, the current research aims at studying the effects of the transverse steel reinforcement inside the concrete slab on the crack control and stress redistribution along the concrete slab.

2. Experimental program

Ten composite beams with mono-symmetric steel cross-sections (B1

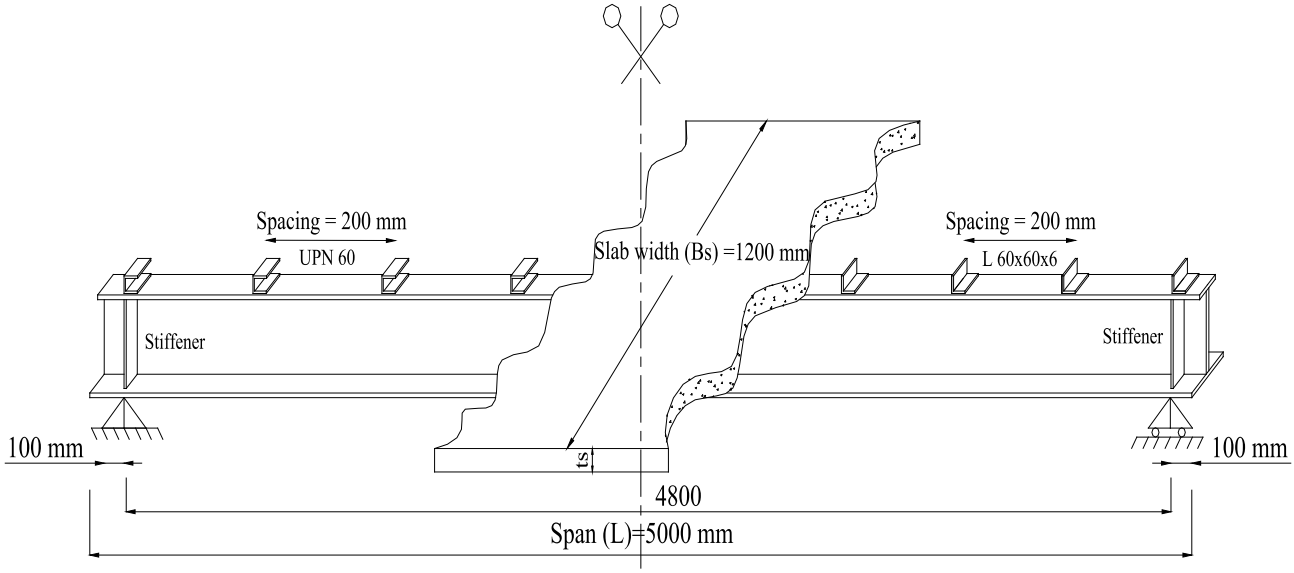

(a) Beam profile

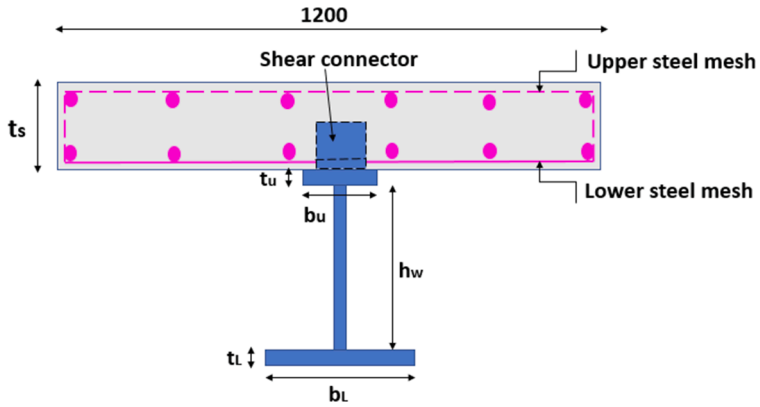

(b) Cross-section

Fig. 1. Test specimens.

to B10) with a total length of 5000 mm are tested in the current experimental program. The beams are simply supported with a clear span of 4800 mm, as shown in Fig. 1. Table 1 illustrates the cross-section dimensions of all tested beams. All beams are fabricated using mono-symmetric steel sections with the area of the lower steel flange double the area of the upper steel flange. The concrete slab width (Bs) is taken as one-quarter of the beam span equal to 1200 mm. A lower steel reinforcement mesh, with steel bars spaced at 200 mm in both the longitudinal and transverse directions, was embedded in the concrete slab, for all tested beams. The diameter of the lower steel bars is 8 mm. Additional upper reinforcement mesh is provided for the concrete slabs of beams B5 and B6. The reinforcement ratio is defined as the total area of steel rebars (i.e., upper and lower steel bars) with respect to the area of the concrete slab ($\rho = A_b/A_c$). The variable parameters studied in this experimental program are the shape of the shear connector (channels or angles), the reinforcement ratio ($\rho = 0.18, 0.21, 0.31, 0.46$ or 0.54), the concrete slab thickness (ts = 80, 120, or 140 mm) and the size of the steel section in terms of the dimensions of its plates. It should be noted that the provided area of the transverse steel reinforcement bars in beams B5 and B6 satisfies the EN 1992–1-1 requirements.

3. Shear connectors

Welded shear connectors are used for all beams, where C-channels (UPN 60) are used for five beams (B1, B3, B5, B7, and B9), and angles (L 60) are used for five beams (B2, B4, B6, B8, and B10). The shear connectors are designed according to Eurocode4; DD ENV 1994–2:2001 equation, clause 6.2.1, where the resistance of the channel shear connector (P_{Rd}), the acting shear force, and the pitch distance (P) between shear connectors are calculated using the following equations:

$$P_{Rd} = \frac{20bh^{\frac{3}{4}}f_{ck}^{\frac{1}{3}}}{\gamma_V} \quad (1)$$

$$Shear\ flow\ at\ yield: q = \frac{Q_y S_x}{I_V} \quad (2)$$

$$Required\ Pitch\ distance: P = \frac{P_{Rd}}{q} \quad (3)$$

Where:

P_{Rd} = is in newtons (N);
b = is the length of the channel in millimeters (mm);
h = is the height of the channel in millimeters (mm);
f_{ck} = is the characteristic cylinder strength of concrete (N/mm^2),
γ_V = is the partial safety factor, should be taken as 1.25 for the ultimate limit state
Q_y = Beam shear force at the yield stage (N),
S_x = Statical moment of area of the concrete slab about the x-x axis (mm^3) and
I_V = Moment of inertia of the composite section about x-x axis (mm^4)

It should be noted that Eurocode 4 provides only one equation for channel shear connector. This equation assumes that the web of the channel is vertical with the shear applied nominally perpendicular to the web. Therefore, this equation is used to estimate the capacity of the angle shear connector.

Table 2 shows the predicted nominal strength of each tested beam. Table 2 lists also the required pitch distance (P) and the degree of composite action for each beam (P/S), where S is the actual pitch distance between connectors and is taken equal to 200 mm.

3.1. Material properties

3.1.1. Concrete

All slabs were cast using normal weight concrete of density equal to 25 kN/m^3. The concrete mix was designed to provide a characteristic strength of 35 MPa. Six concrete cubes were cast alongside the beams, weighted, and tested on the same day of the corresponding beam test to determine the actual concrete compressive strength.

3.1.2. Steel section and reinforcement rebars

Samples from the steel plates and the reinforcement bars were taken and tested in the laboratory. The yield stress, ultimate stress, Young's modulus, and the percentage of elongation values for each sample are shown in Table 3.

3.2. Preparation of specimens

The web and flange plates were assembled together for each beam using a 6 mm welding size. The shear connectors were welded to the upper flanges, as shown in Fig. 2(a), with a constant spacing equal to 200 mm for all beams. Wooden forms were prepared to cast the concrete slabs above the steel beams. The steel reinforcement meshes were then

Table 2
Design of Shear Connectors according to Eurocode 4; CEN 2004.

Beam ID	Ultimate load (kN)	I_v (mm^4) x10^4	P_{Rd} (kN)	P(mm)	Degree of composite action, P/S
B1	454.29	23,725	99.49	167.40	0.84
B2	454.29	23,725	99.49	163.05	0.82
B3	599.13	34,709	99.49	193.10	0.97
B4	550.85	30,779	99.49	169.18	0.85
B5	599.13	35,288	99.49	185.16	0.93
B6	550.85	31,301	99.49	171.40	0.86
B7	223.33	11,773	78.55	207.04	1.04
B8	223.33	11,773	78.55	211.61	1.06
B9	134.00	6045	57.60	231.02	1.16
B10	134.00	6045	57.60	233.35	1.17

Table 1
Details of Tested Specimens.

Beam ID	Slab thickness, t_s (mm)	Reinforcement Ratio A_b/A_c (%)	Type of Shear Connector	Lower Flange		Web		Upper Flange		Radius of gyration of steel, r_s (mm)
				b_L (mm)	t_L (mm)	h_w (mm)	t_w (mm)	b_u (mm)	t_u (mm)	
B1	80	0.31	UPN 60	200	12	260	8	100	12	113.74
B2		0.31	Angle 60							
B3	140	0.18	UPN 60							
B4	120	0.21	Angle 60							
B5	140	0.46	UPN 60							
B6	120	0.54	Angle 60							
B7	80	0.31	UPN 60	160	10	200		80	10	86.64
B8			Angle 60							
B9			UPN 60	120		150	6	60		67.70
B10			Angle 60							

Table 3
Mechanical properties of steel plates and steel reinforcement.

Steel Section	Yield Stress, f_y (MPa)	Ultimate Stress, f_u (MPa)	Young's Modulus, E (GPa)	Elongation at ultimate %
Plate 6 mm	275	470	210	27
Plate 8 mm	290	470	210	28.3
Plate 10 mm	320	550	210	21.97
Plate 12 mm	360	550	210	21
Diameter 8 mm	350	435	200	13.6
Diameter 10 mm	490	570	200	14.1

placed in wooden forms, as shown in Fig. 2(b). The concrete was poured, compacted, and leveled, as shown in Fig. 2(c). The concrete slabs were continuously moistured with water for seven days and kept in the atmospheric temperature of the laboratory for four weeks before testing.

3.3. Instrumentations

The displacements were measured using five LVDTs with a maximum stroke of 100 mm and an accuracy of 0.01 mm. Three LVDTs were mounted to record the vertical deflection of the steel beam and the concrete slab at the beam mid-span, as shown in Fig. 3(a). Another two horizontal LVDTs were used at the two ends of the beams to record the horizontal displacement (slip) at the interface between the concrete slab and the steel beam. Nine strain gauges were used, in the current test, to record the strains at different locations during the experiment. The length and resistance of all strain gauges are 100 mm and 120 Ohm, respectively. Five strain gauges were attached to the concrete slab, one strain gauge was attached to the embedded steel reinforcement bar and finally, three strain gauges were attached to the steel beam. Gauges (ε_{c1} to ε_{c4}) were attached to the upper surface of the concrete slab to record the compression strain distribution along the concrete width at the mid-span section, as shown in Fig. 3 (b), and the fifth strain gauge (ε_{c5}) was attached to the bottom side of the concrete slab right beside the upper steel flange. Gauges (ε_{s1} to ε_{s3}) were attached to the mid-span section, at the upper and lower flanges of the steel beam as well as at the mid-height of the steel web, as shown in Fig. 3 (c). The ninth strain gauge was attached on the transverse steel rebars of the upper steel reinforcement mesh for beams B5 and B6 only, as shown in Fig. 3 (d).

3.4. Test procedure

The specimens were mounted and adjusted in the loading frame and were loaded using a rigid spreader beam to allow for a four-point loading setup, as shown in Fig. 3(a). The specimens were tested using a 2000 kN capacity hydraulic jack with 5.0 kN accuracy.

4. Experimental results

The results of the tested beams are plotted in terms of load versus vertical deflection at mid-span in Fig. 4, slip at the interface between steel and concrete slab in Fig. 5, strains of lower steel flange in Fig. 6, upper and lower strains of the concrete slab in Fig. 7, strains at the transverse steel rebars of the upper reinforcement mesh in Fig. 8, location of the neutral axis in the concrete slabs in Fig. 9 and the strain profile of the mid-span cross sections at both the yield and ultimate loads in Fig. 10.

Besides, Table 4 lists the load values at the initiation of yield, transverse cracks, longitudinal cracks, and ultimate. The table lists also the vertical deflections at yielding and ultimate loads as well as the horizontal slip at the steel–concrete interface at the elastic and ultimate stages.

The yielding load is determined when the longitudinal strain at the underside of the lower steel flange (ε_{s3}) reaches the yielding strain value. The yielding strains of the steel plates, based on the tested coupons, are

(a) Welding of shear connectors

(b) Formwork and reinforcement mesh

(c) Concrete pouring.

Fig. 2. Fabrication of beams.

0.171% for beams B1 to B6 and 0.152% for all other beams.

4.1. Effect of the shear connector type

In this section, the flexural behaviour of three pairs of beams is presented to determine the effects of changing the type of shear

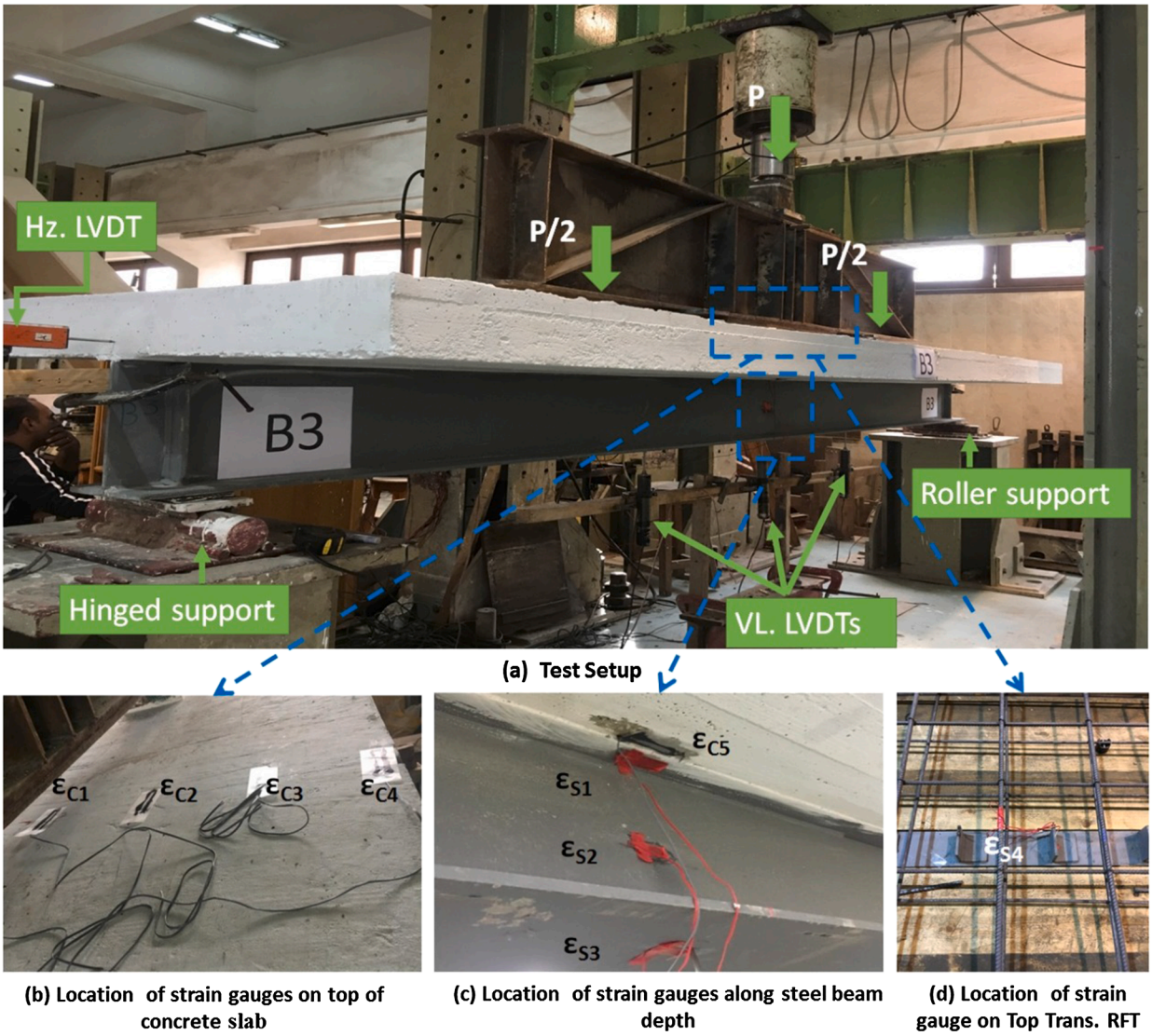

Fig. 3. Test setup and instrumentations.

connectors (i.e., channels or angles). Pair 1 (beams B1 and B2) is the only pair of these pairs which have partial composite action with a P/S value equal to 0.83, as indicated in Table 2. The other two pairs of beams (pairs 2 and 3) have full composite action with a P/S value greater than one.

Beams B1 and B2 (pair 1), are identical beams except for the used type of shear connectors. The radius of gyration of the steel section for pair 1 equals 113.74 mm. B1 is provided with channel shear connectors (UPN 60), while B2 is provided with angle shear connectors (L 60). Although using different shapes of shear connectors the two beams reached almost the same yielding and ultimate load levels, as shown in Table 4. The yielding loads for beams B1 and B2 are 375 kN and 385 kN, respectively. The failure loads are 457.67 kN and 459.93 kN for beams B1 and B2, respectively.

Table 4 shows that the difference between the slip values at the interface between the concrete slab and the steel beam is higher at the elastic stage before yielding of steel. Table 4 lists slip values for B1 and B2 at the elastic limits as 0.23 mm and 0.33 mm, respectively. These values indicate that the channel shear connectors were 30% stiffer than the angle shear connectors in resisting the slip of concrete slab within the elastic range. Therefore, when the concept of partial composite action is adopted in the design of composite beams it is recommended to use channel connectors to reduce the slip rate of the concrete slab.

Fig. 9 shows the location of the neutral axis with respect to the concrete slab. The location is calculated based on the strain values at the top surface of the concrete slab (ε_{c1}) and the strain values at the bottom surface of the concrete slab (ε_{c5}). Also, the figure shows the load value at which the underside concrete crack started to propagate. The underside concrete crack occurred at a concrete strain value of 100 μ strain, which is corresponding to the allowable tensile strength of concrete with a compressive strength of 35 MPa. Fig. 9(a) shows that beam B1 with channel connectors exhibited a gradual increase in the tension zone of the concrete slab with increasing the load until beam failure occurred. Beam B2 with angle connectors experienced earlier initiation of tension stresses in the concrete slab with a similar rate for the neutral axis shift until the depth of the neutral axis reached 7.6 mm inside the concrete slab. It should be noted that this point marks the initiation of yielding strains at the steel cross-section (Py = 385 kN). The neutral axis depth was then stabilized before experiencing a noticeable jump inside the concrete slab until it reached a depth of 35.2 mm before beam failure occurs.

B7 and B8 are another identical pair (pair 2) of beams with a smaller steel cross-section than those of pair 1. The radius of gyration of pair 2 equals 86.64 mm. The measured yield loads for beams B7 and B8 are 185 kN and 181 kN, respectively, as shown in Table 4. A higher difference is measured in the ultimate load capacity between both beams. The failure

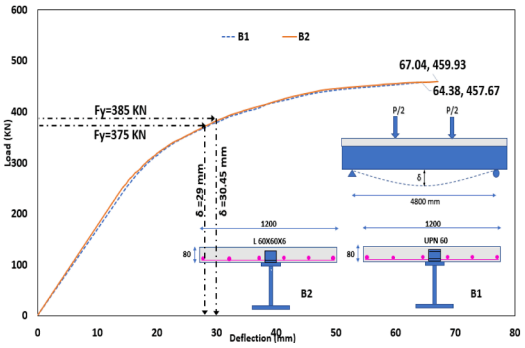

(a)Beams B1 & B2-effect of shear connectors

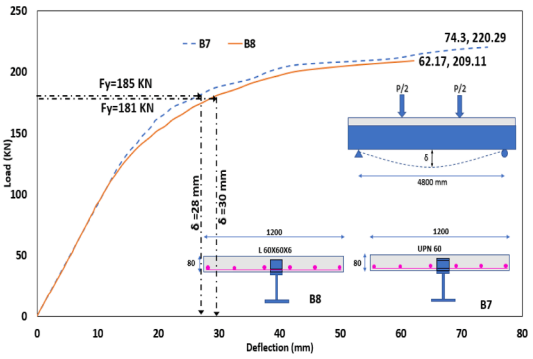

(b) Beams B7 & B8-effect of shear connectors

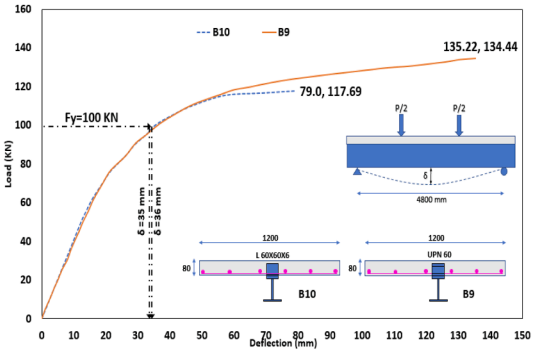

(c) Beams B9 & B10-effect of shear connectors

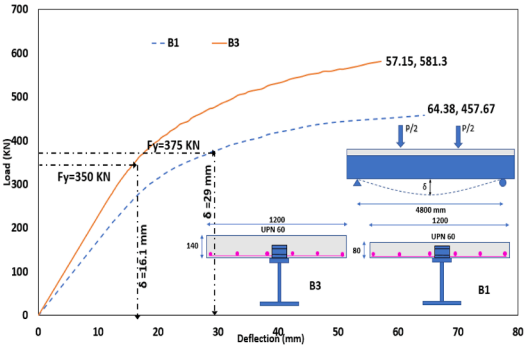

(d) Beams B1 & B3-effect of slab thickness (channel)

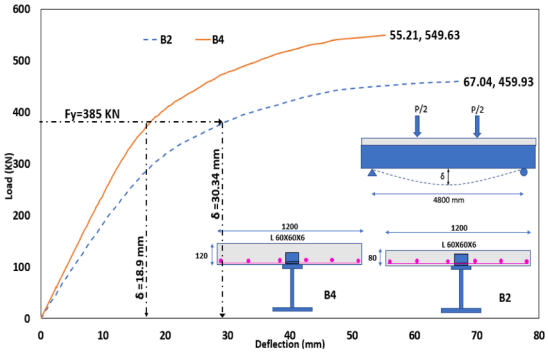

(e) Beams B2 & B4-effect of slab thickness (angle)

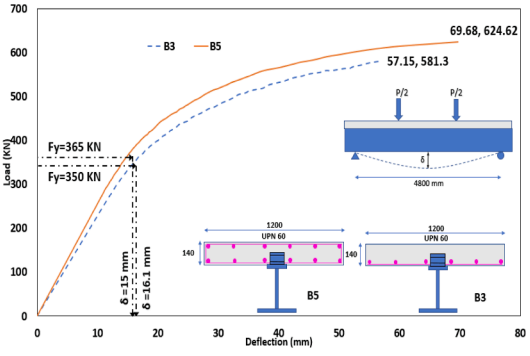

(f) Beams B3 & B5-effect of slab top RFT (channel)

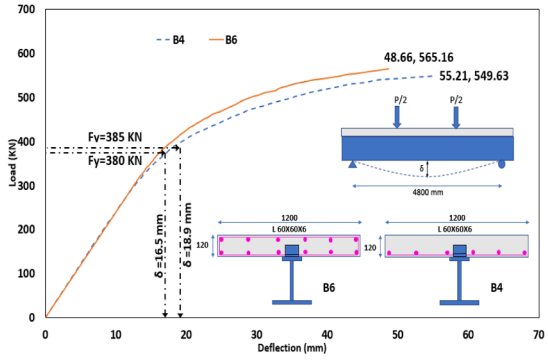

(g) Beams B4 & B6-effect of slab top RFT (angle)

Fig. 4. Load-deflection curves of all tested beams.

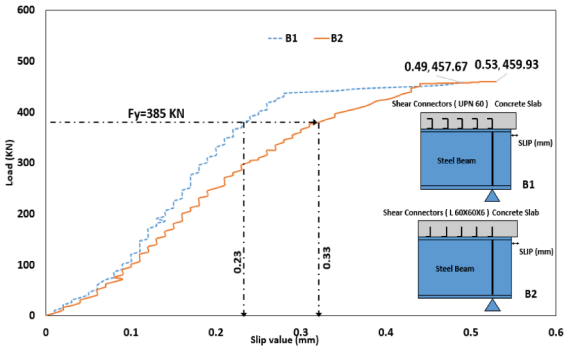

(a) Beams B1 & B2-effect of shear connectors

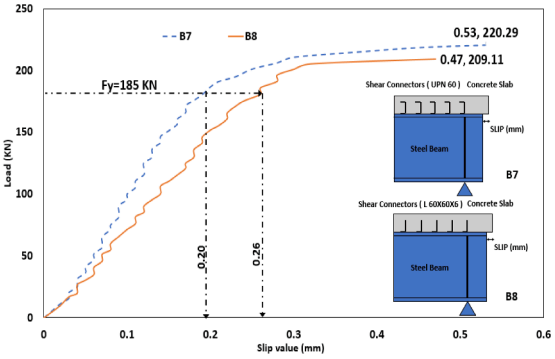

(b) Beams B7 & B8-effect of shear connectors

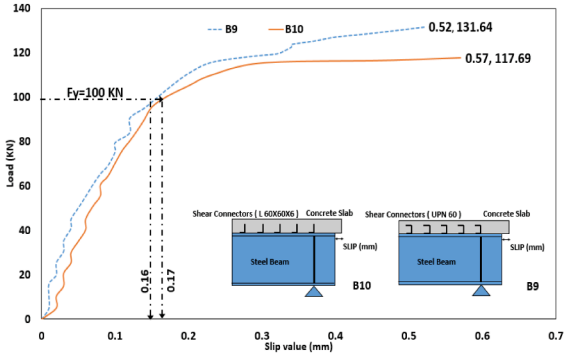

(c) BeamsB9 & B10-effect of shear connectors

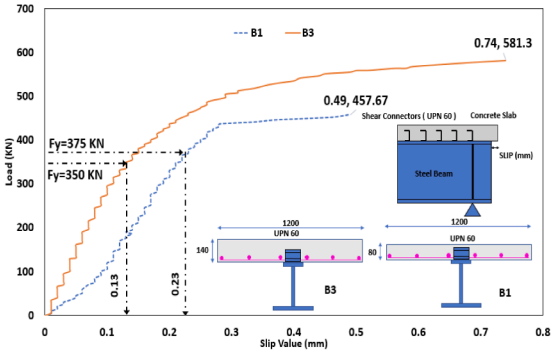

(d) Beams B1 & B3-effect of slab thickness (channel)

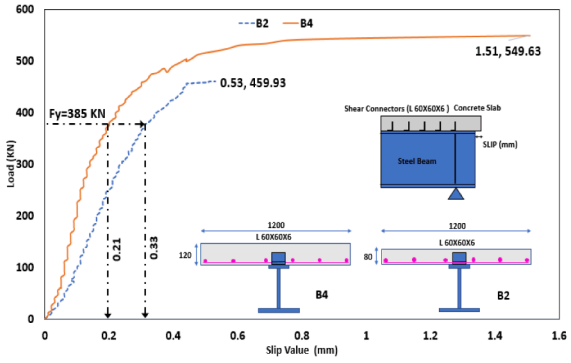

(e) Beams B2 & B4-effect of slab thickness (angle)

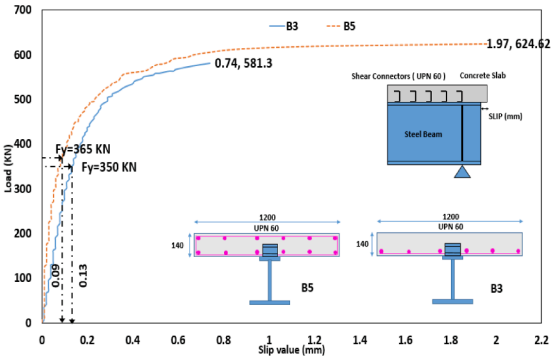

(f) Beams B3 & B5-effect of slab top RFT (channel)

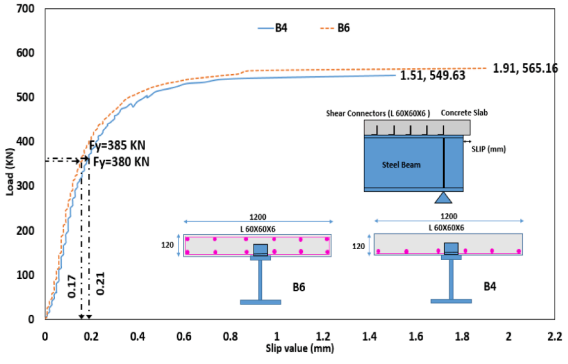

(g) Beams B4 & B6-effect of slab top RFT (angle)

Fig. 5. Load-slip of concrete slab of all tested beams.

loads for beams B7 (with channels) and B8 (with angles) are 220.29 kN and 209.11 kN, respectively, which indicate 5% enhancement for B7. Fig. 5(b) shows that the slip values at the elastic limits for B7 and B8 are 0.20 mm and 0.26 mm, respectively. These values indicate that the channel shear connectors recorded the same increase in stiffness (30%) in resisting the slip of concrete slab within the elastic range. These shear connectors in this pair of beams are classified to just provide the full composite action with P/S values are 1.02 and 1.07 for beams B7 and B8,

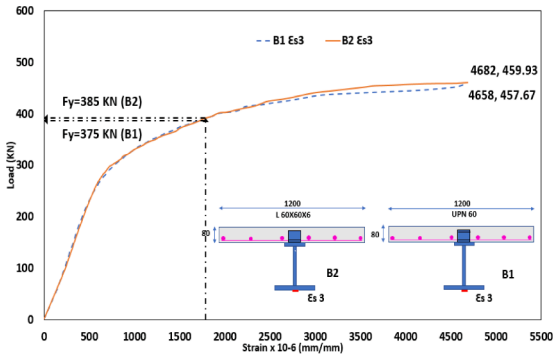

(a) Beams B1 & B2-effect of shear connectors

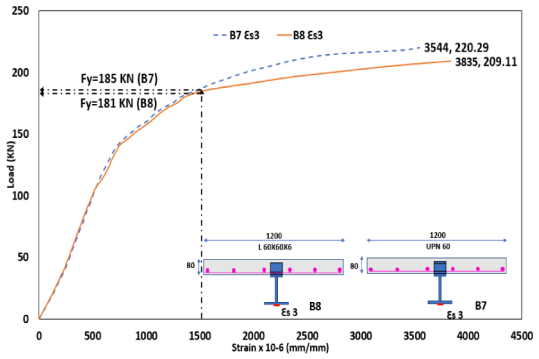

(b) Beams B7 & B8-effect of shear connectors

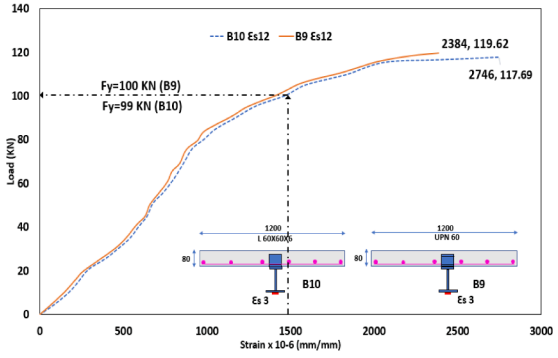

(c) Beams B9 & B10-effect of shear connectors

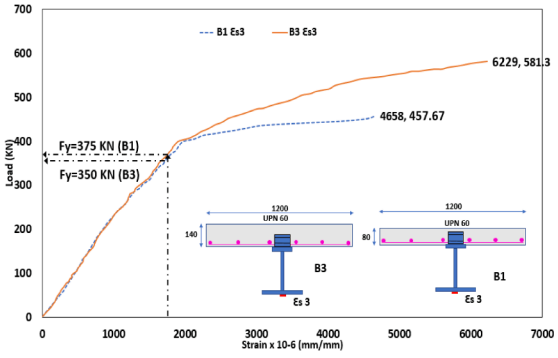

(d) Beams B1 & B3-effect of slab thickness (channel)

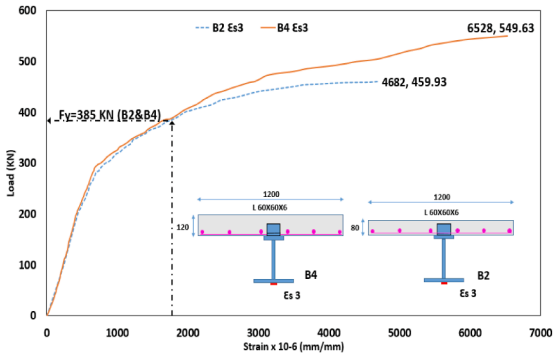

(e) Beams B2 & B4-effect of slab thickness (angle)

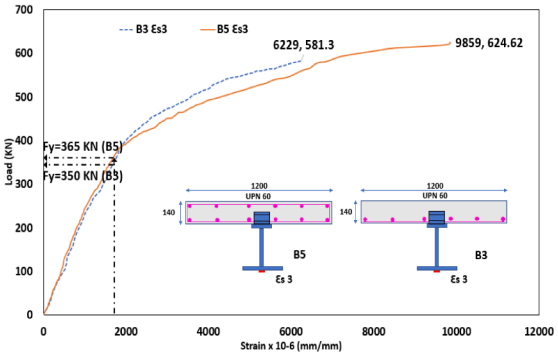

(f) Beams B3 & B5-effect of slab top RFT (channel)

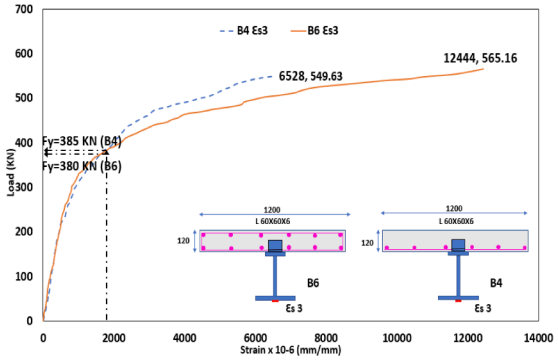

(g) Beams B4 & B6-effect of slab top RFT (angle)

Fig. 6. Load-strains at the steel lower flange (ε_{s3}) of all tested beams.

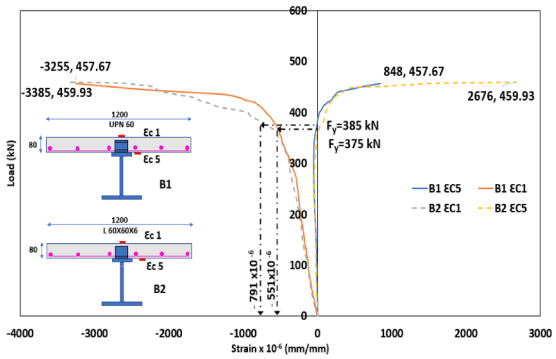

(a) Beams B1 & B2-effect of shear connectors

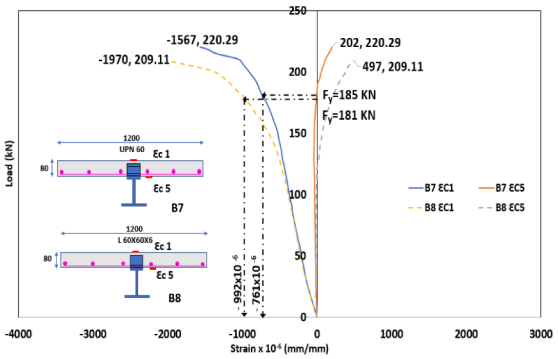

(b) Beams B7 & B8-effect of shear connectors

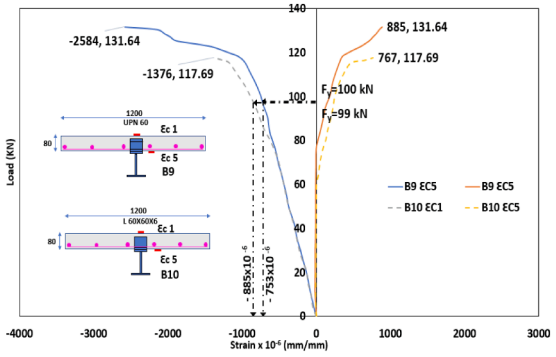

(c) Beams B9 & B10-effect of shear connectors

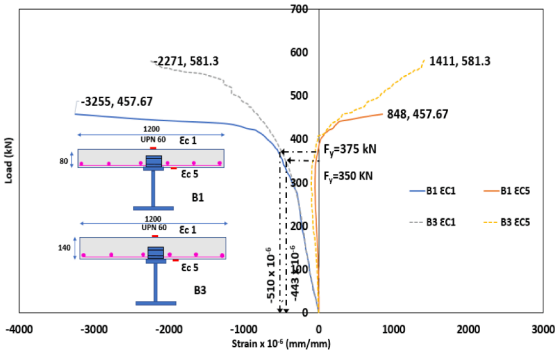

(d) Beams B1 & B3-effect of slab thickness (channel)

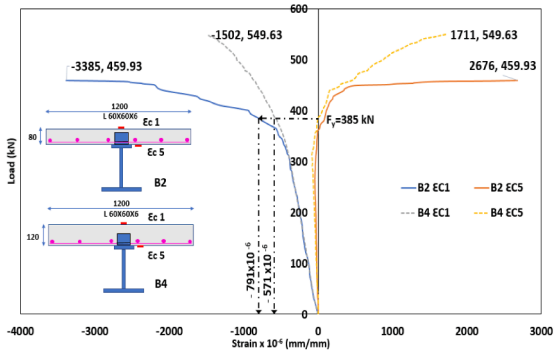

(e) Beams B2 & B4-effect of slab thickness (angle)

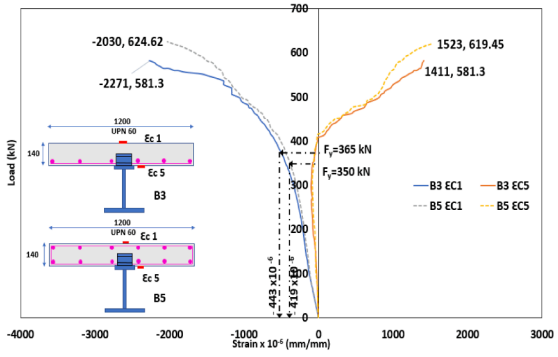

(f) Beams B3 & B5-effect of slab top RFT (channel)

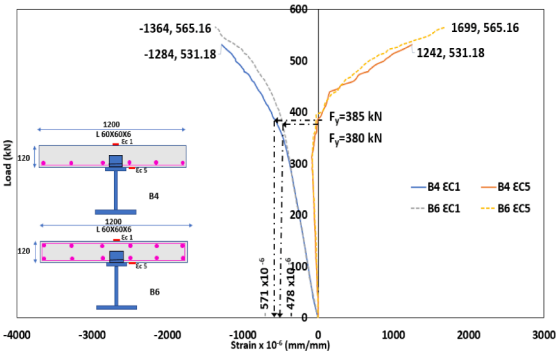

(g) Beams B4 & B6-effect of slab top RFT (angle)

Fig. 7. Load-upper & lower strains of concrete slab (ε_{c1}, ε_{c5}) of all tested beams.

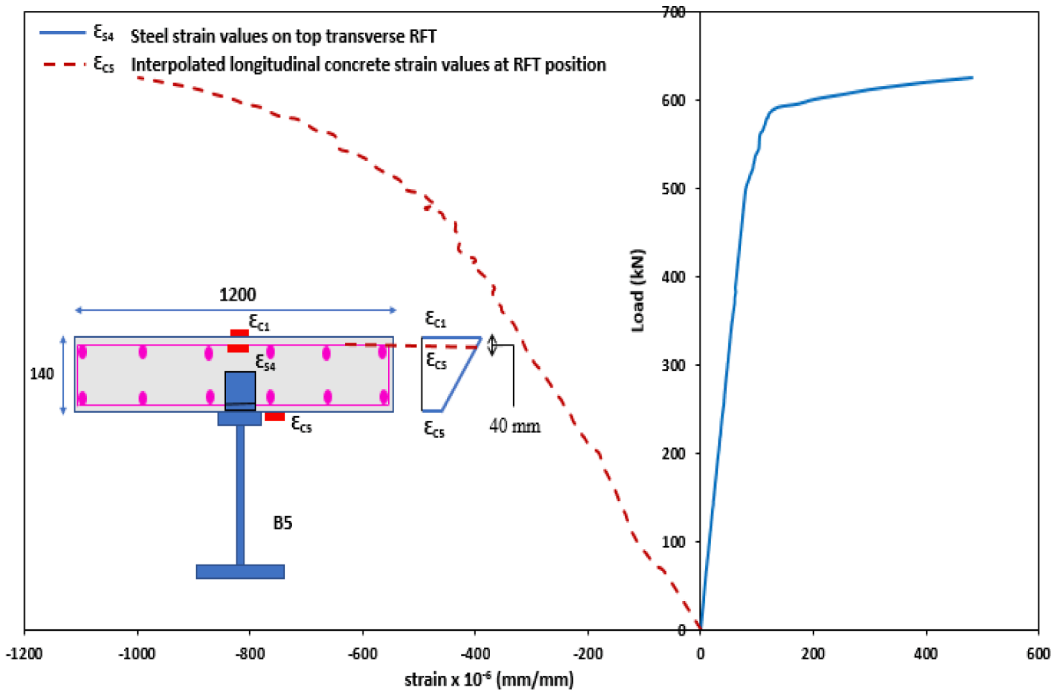

(a) Load-strain at Beam (B5)

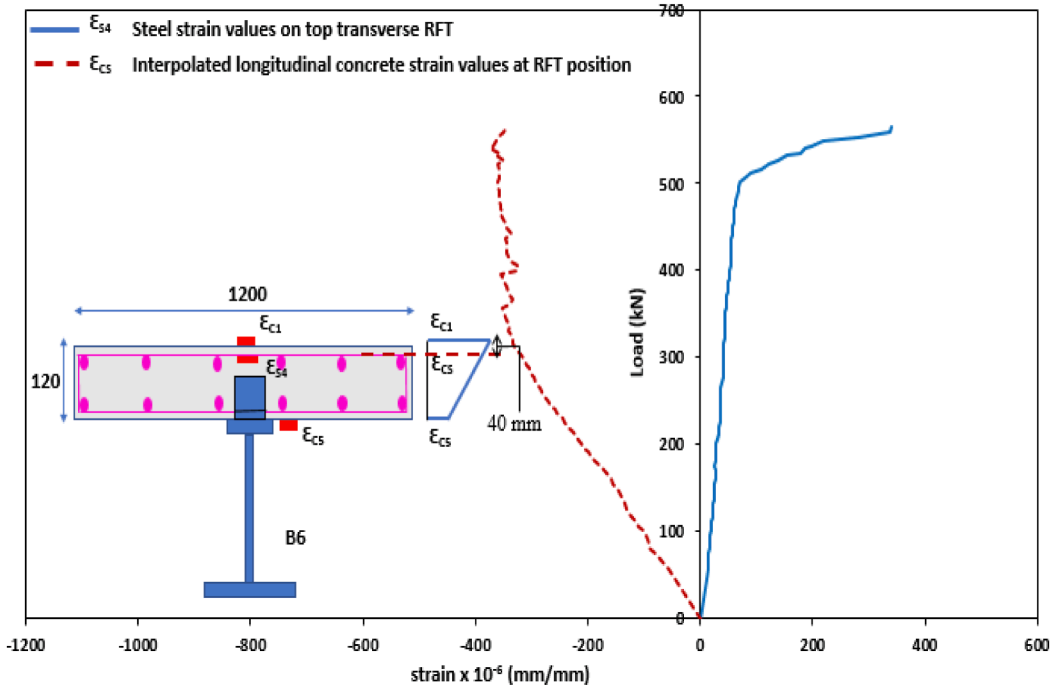

(b) Load-strain at beam (B6)

Fig. 8. Load versus strain at the upper transverse reinforcement steel.

respectively.

Fig. 9(d) shows that beam B8 with angle connectors experienced earlier initiation of tension in concrete slab than that of beam B7 with channel connectors. Both beams experienced a gradual increase in the tension zone until failure.

Beams B9 and B10 are the 3rd pair (pair 3) with full-composite action, where P/S values are 1.14 and 1.19, respectively. The steel section size of this pair is the smallest among all tested specimens, where the radius of gyration of the steel section is 67.70 mm. The measured yield loads for beams B9 and B10 are 100 kN and 99 kN, respectively, as shown in Table 4. The difference in the ultimate load capacities between both beams becomes obvious in this case, where the failure loads are 134.44 kN and 117.69 kN for beams B9 and B10, respectively, which indicate 14% enhancement for B9. Fig. 5(c) shows that the slip values at the elastic limits for B9 and B10 are 0.16 mm and 0.17 mm, respectively, which represents a very small effect for the type of shear connector. These observations indicate that the effect of using channels as shear connectors on the ultimate strength is higher for full composite action

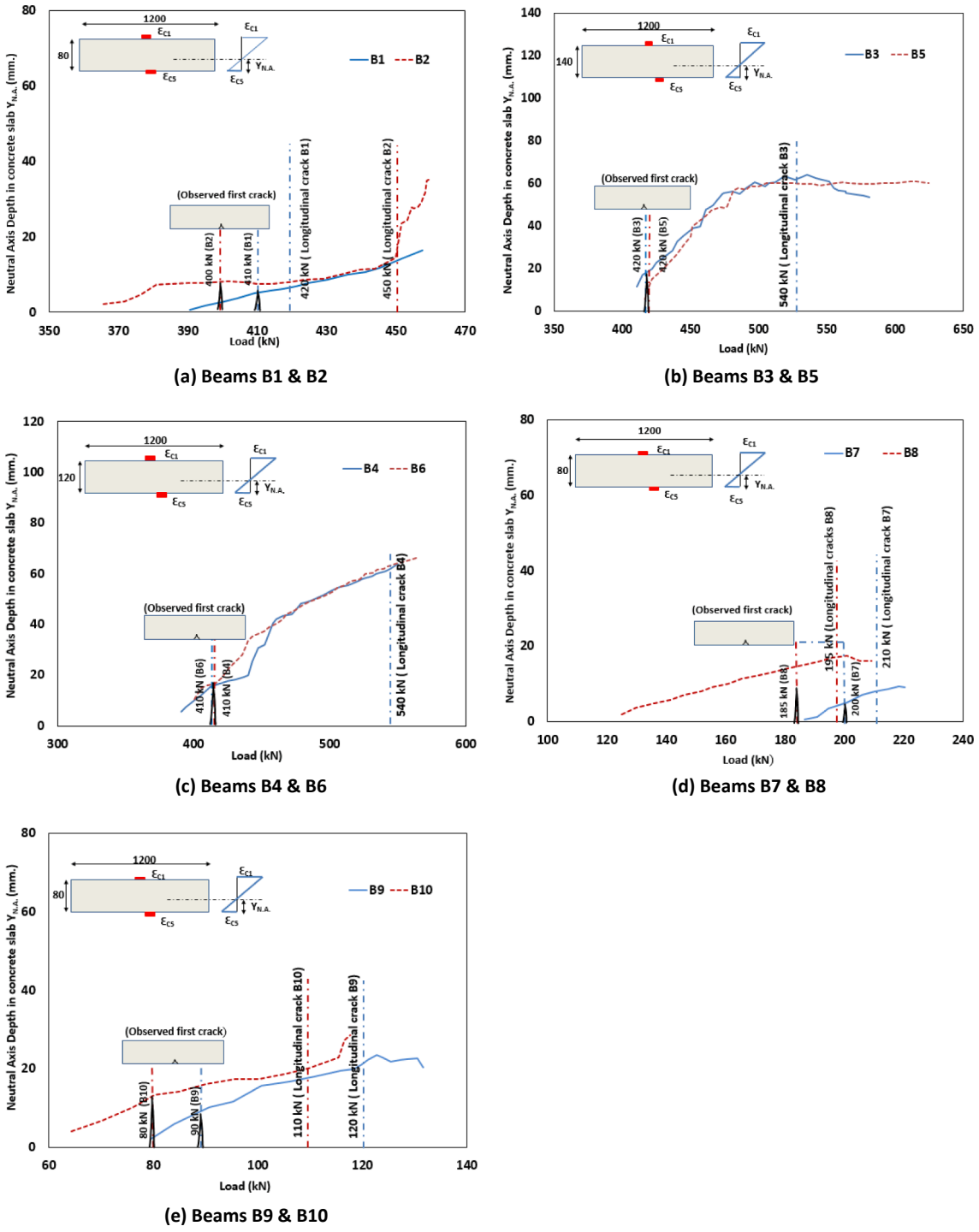

Fig. 9. Load versus neutral axis depth in concrete slab.

beams, while its effect on the slip values is higher for partial composite action beams.

Fig. 9(e) shows that beam B10 with angle connectors experienced the same earlier initiation of tension in concrete slab compared to beam B9 with channel connectors. Both beams experienced a gradual increase in the tension zone until failure.

Fig. 10 shows the strain profiles for beams (B1, B2), (B7, B8), and (B9, B10). For all six beams, strain compatibility was maintained and the cross-sections of the composite beams remained plane up to the level of yield loads, regardless the shear connector type or the degree of composite action. Beyond the yield loads and up to the ultimate loads, incompatible strain values were observed at the interface between the concrete slabs and steel cross-sections with higher values of incompatibility for composite beams with angle type of shear connectors associated with partial composite action (i.e., B2).

4.2. *Effect of the concrete slab reinforcement ratio*

In this section, the results of two pairs of composite beams (B3, B5) and (B4, B6) are presented to determine the effects of the steel reinforcement ratio of the concrete slab on the behaviour of composite beams.

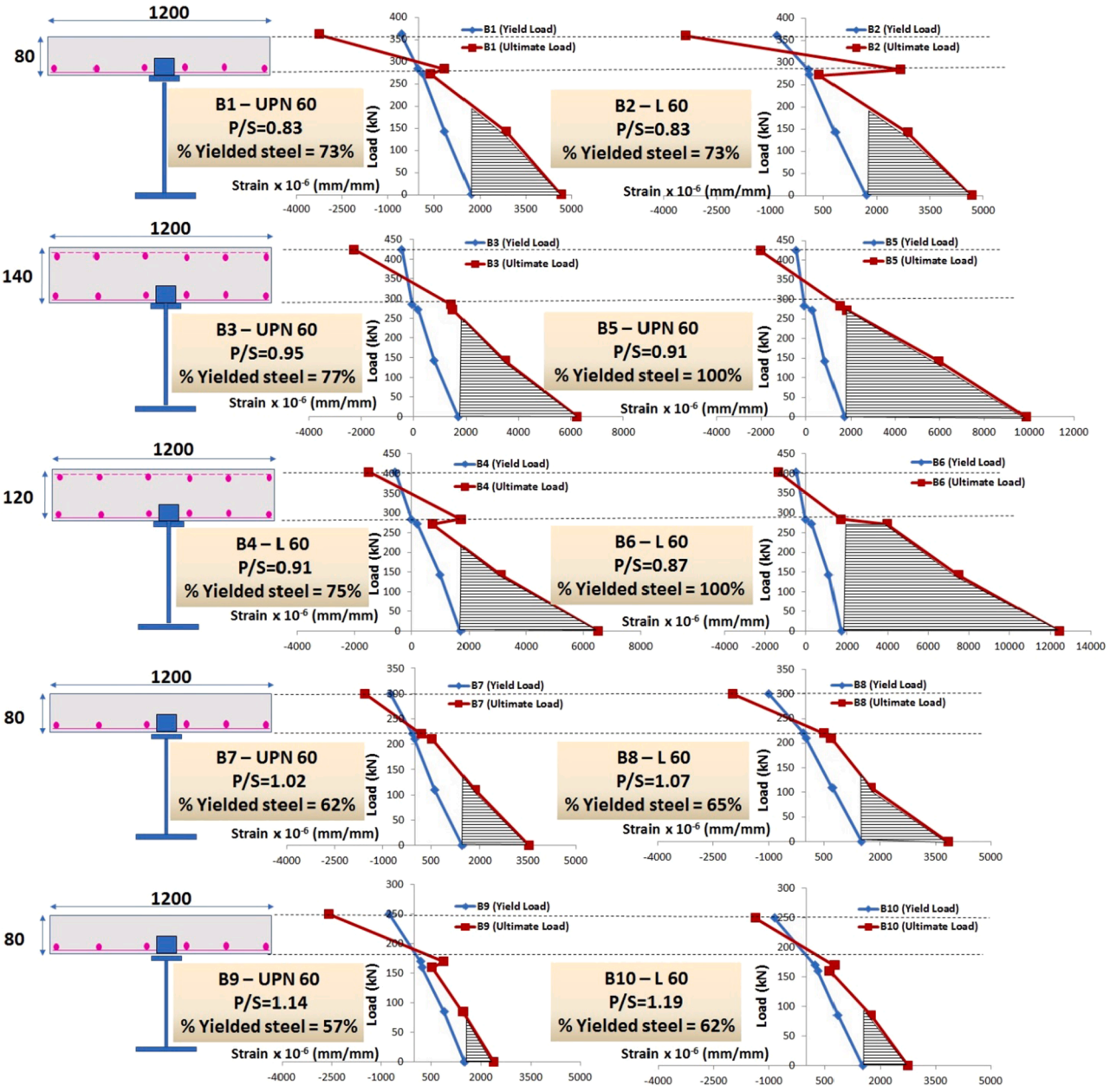

Fig. 10. Effect of shear connector type on Strain distribution.

Table 4
Summary of test results.

Beam ID	Elastic Stage (Yield)			Load at transverse cracks (kN)	Load at longitudinal cracks (kN)	Ultimate Stage		
	P_y (kN)	Deflection δ_y (mm)	Slip (mm)			P_u (kN)	Deflection δ_u (mm)	Slip (mm)
B1	375	29	0.23	410	420	457.7	64.38	0.49
B2	385	30.45	0.33	400	450	459.9	67.04	0.53
B3	350	16.1	0.15	420	540	581.3	57.15	0.74
B4	385	18.9	0.21	410	540	549.6	55.21	1.51
B5	365	15	0.08	420	N/A	624.6	69.68	1.97
B6	380	16.5	0.18	410	N/A	565.2	48.66	1.91
B7	185	28	0.2	200	210	220.3	74.3	0.53
B8	181	29.9	0.26	185	195	209.1	62.17	0.47
B9	100	36	0.16	90	120	134.4	135.22	0.52
B10	99	34.5	0.17	80	110	117.7	79.02	0.57

Beams B3 and B5 are identical beams except for the reinforcement ratio of the concrete slab. Beams B3 and B5 (with 140 mm thick concrete slabs) have reinforcement ratios (Area of longitudinal steel rebars with respect to the area of the concrete slab, A_b/A_c) equal to 0.18% and 0.46%, respectively. It should be noted that these two beams are provided with channel connectors.

Fig. 11 shows the strain distribution at the upper side of the concrete slab. Fig. 11(a) indicates a better strain distribution in the concrete slab at the transverse direction when using higher reinforcement ratios at both the elastic and ultimate stages. The effect is more pronounced at the ultimate stage, where the ratio of the strain at the centerline of the slab divided by the strain at the slab edge ($\varepsilon_{c1}/\varepsilon_{c4}$) equals 3.6 and 1.1 for beams B3 and B5, respectively. The fairly uniform strain distribution at the top of the concrete slab in the case of beam B5 is believed to increase the effective concrete slab and hence improve the behaviour of the composite beam. This is attributed to the presence of the transverse steel reinforcement in the concrete slab. The transverse steel reinforcement reduces shear lag phenomena by preventing the presence of the top longitudinal concrete cracks.

As shown in Table 4, beams B3 and B5 failed at 581.3 kN and 624.6 kN, respectively, which indicates a 7.45% increase in flexural strength due to the increase in slab reinforcement ratio. The measured yield loads for beams B3 and B5 are 350 kN and 365 kN, respectively, which indicates a 4.3% increase in the yield load due to the increase in slab reinforcement ratio. In addition, it is noted that steel reinforcement of the concrete slab has a significant impact on the deflection of the composite beam, especially at the ultimate load stage. Increasing the reinforcement ratio of the concrete slab from 0.18% (B3) to 0.46% (B5), the

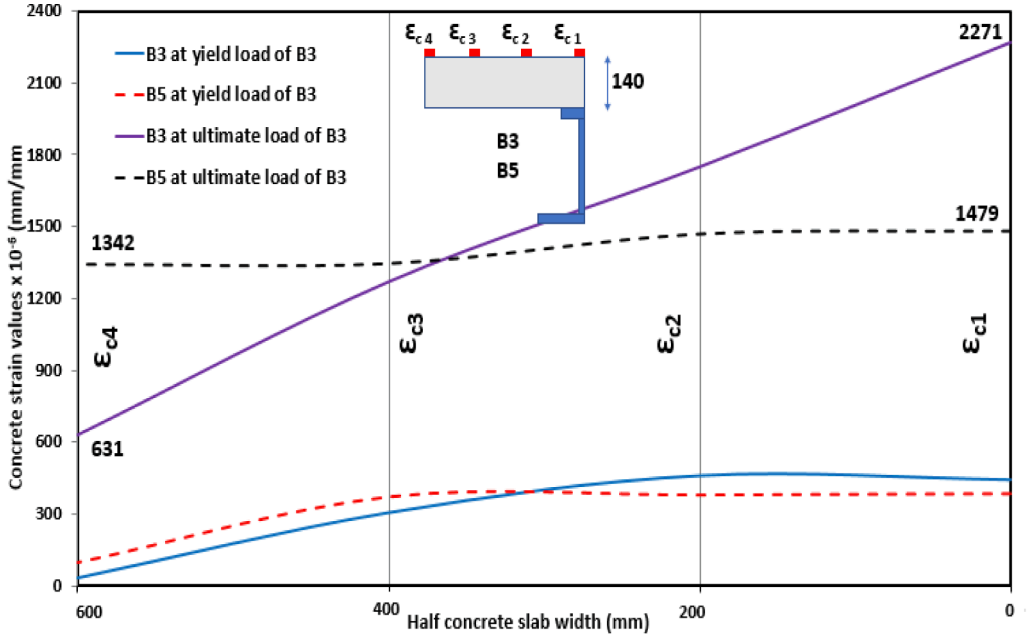

(a) Strain distribution for beams B3 and B5

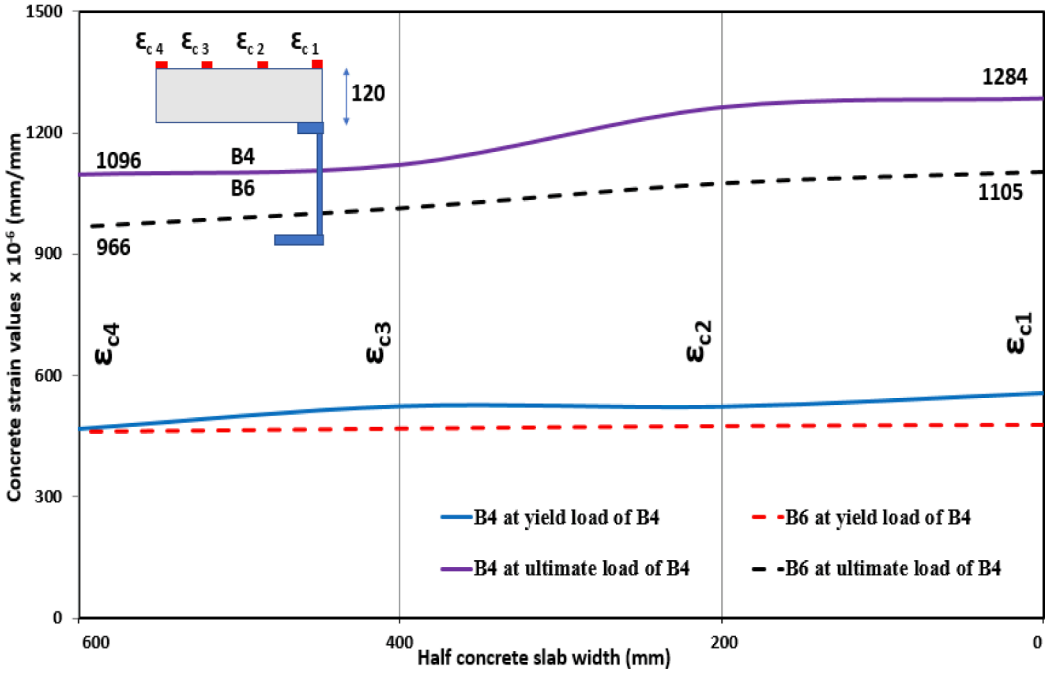

(b) Strain distribution for beams B4 and B6

Fig. 11. Strain distribution a long the concrete slab.

deflection values of composite beams are dropped by 7% and 23% at the yielding and ultimate loads of B3 (350 kN and 581.3 kN), respectively.

Fig. 8 shows a comparison between the calculated longitudinal strain values in the concrete slab (ε_{cs}) and the transverse strain values in the upper steel mesh (ε_{s4}). the longitudinal strain values in the concrete slab (ε_{cs}) are calculated by interpolation between the measured strains (ε_{c1} & ε_{c5}). The transverse strain values at the upper reinforcement mesh are way below their yielding strain, as shown in Fig. 8. The absolute ratio of the longitudinal strain over the transverse strain values ($\varepsilon_{s4}/\varepsilon_{cs}$), known also as Poisson's ratio, is calculated throughout the test of beam B5 and plotted in Fig. 12(a). The figure shows almost a constant value for Poisson's ratio equal to 0.16 throughout the test before increasing up to a value of 0.5 at the failure load.

Beams B4 and B6 are identical beams except for their concrete slab reinforcement ratios. Beams B4 and B6 have reinforcement ratios (A_b/A_c) equal to 0.21% and 0.54%, respectively. Also, Beams B3 and B5 are identical except for their slab reinforcement ratios. It can be noted that B4 and B6 have a concrete slab reinforcement ratio higher than B3 and B5. The ratio of slab reinforcement of B6 to B4 and B5 to B3 is equal to 2.5. Fig. 11(b) indicates that the strain values of the thin concrete slab (120 mm for beams B4 and B6) are lower than the values of thicker slabs (140 mm for beams B3 and B5). Moreover, the ratio of the strain at the slab centerline divided by the strain at the slab edge ($\varepsilon_{c1}/\varepsilon_{c4}$) equals 1.17 and 1.14 for beams B4 and B6, respectively. These values indicate that the effect of the slab reinforcement ratio on the strain distribution is reduced due to the small strain values developed in thin concrete slabs.

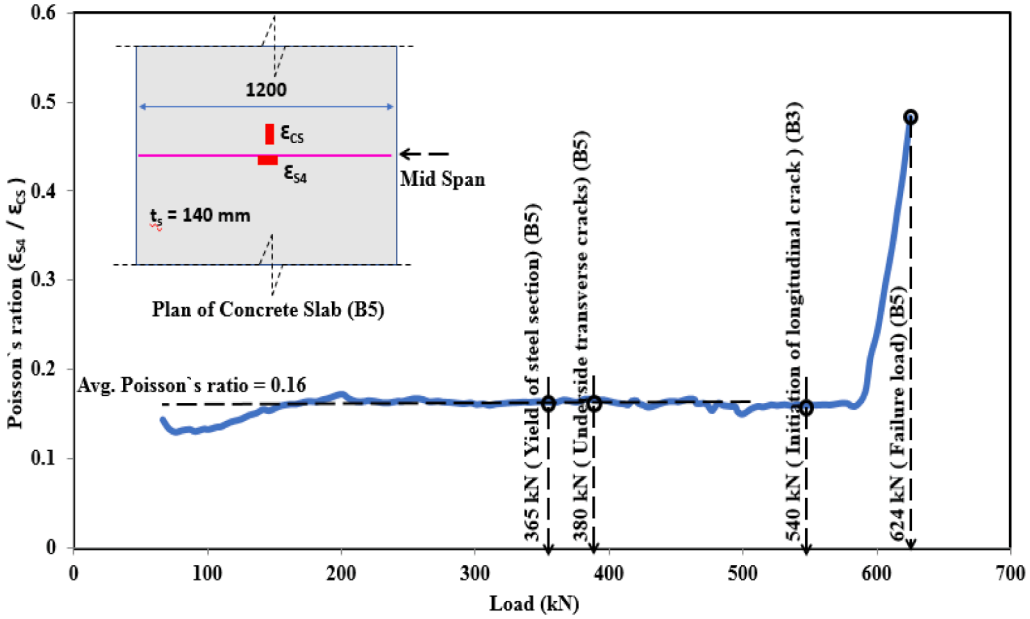

(a) Poisson's ratio for beam (B5)

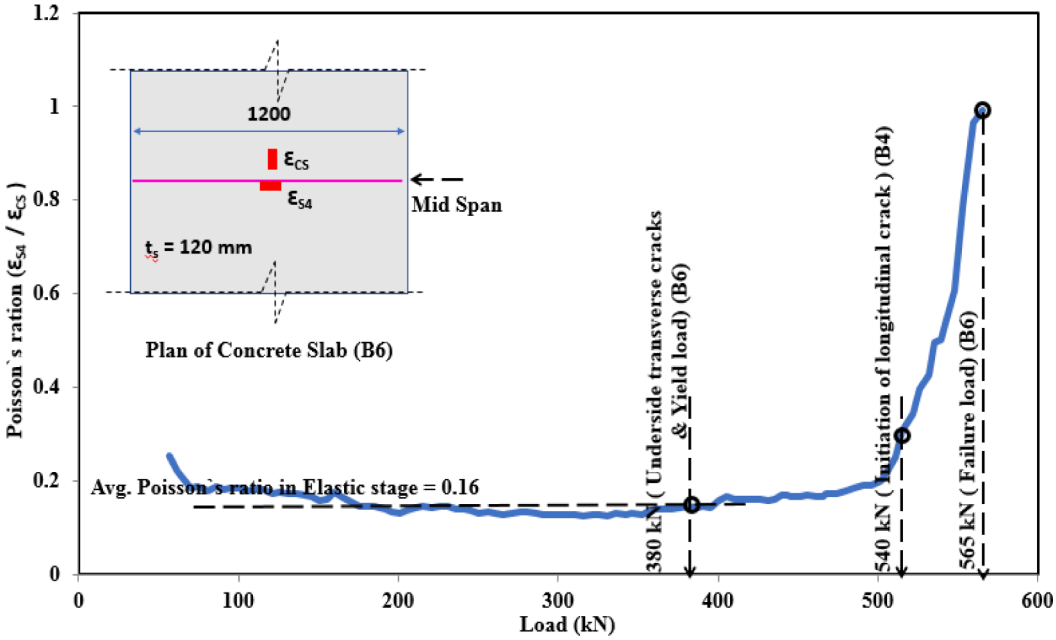

(b) Poisson's ratio for beam (B6)

Fig. 12. Poisson's ratio for the concrete slab.

The measured yield loads for beams B4 and B6 are 385 kN and 380 kN, respectively, as shown in Table 4. Although beam B6 started yielding before beam B4 it failed at a load higher than beam B4. Beams B4 and B6 failed at 549.63 kN and 565.16 kN, respectively, which indicates a 2.8% increase in flexural strength due to the increase in slab reinforcement ratio. In addition, it is also indicated that when increasing the reinforcement ratio of the concrete slab from 0.21% to 0.54%, the deflection values of the composite beams are dropped by 4.5% and 23.7% at the yielding and ultimate loads of B4 (385 kN and 549.63 kN), respectively. Fig. 12(b) shows also a constant value for Poisson's ratio of beam B6 equal to 0.16 throughout the test before increasing up to a value of 1.0 at the failure load.

The measured yield loads for beams B3 and B5 are 350 kN and 365 kN, respectively, as shown in Table 4. The recorded ultimate loads for beams B3 and B5 are 581.3 kN and 624.6 kN, which indicates a 7.4% increase in flexural strength due to the increase in slab reinforcement ratio. Although, the reinforcement slab ratio between beams B6 to B4 is almost the same as beams B5 to B3, beams B5 to B3 recorded a higher difference in ultimate load than B6 to B4. This may be attributed to the type of the used shear connector, as beams B3 and B5 are provided with channel shear connectors, while beams B4 and B6 are provided with angle. The slip values for beams B3 and B4 at failure load are 0.74 and 1.51 mm. While, the slip values for their identical beams B5 and B6, with higher reinforcement slab ratios, at failure load are 1.97 and 1.91 mm. This indicates that the increase in the slab reinforcement in the case of beams provided with channel shear connector enhances the ductility of beams than that beams provided with angle shear connector. Where the ductility ratio (i.e., $\boldsymbol{\delta_u \backslash \delta_y}$) of beams B3, B4, B5 and B6 are 3.56, 2.92, 4.64, and 2.95, respectively.

On the other hand, the increase in the reinforcement ratios has almost a negligible effect on the location of the neutral axis and tension zones at the bottom side of the concrete slab, as shown in Fig. 9(b & c) for beams B3 to B6.

4.3. Failure modes

The failure modes can be divided into three groups with regard to the failure sequence. All load levels associated with failure signs (i.e., the initiation of yielding at the steel section, initiation of transverse and longitudinal cracks in the concrete slab as well as the failure loads) are listed in Table 4. The failure loads for all tested beams show good agreement with the strength predictions according to EC4. Although beams (B1 to B6) are provided with partial composite action according to Eurocode, no signs for the failure of shear connectors were observed until the end of the test. This is probably attributed to the higher strength of all the shear connectors, welded to the steel beam in the zone between the maximum and zero shear, than the least strength of either the steel section or the concrete slab.

Group 1 includes six beams (B1 to B4, B7, and B8), where the steel sections started yielding at the bottom steel flanges. The loading resistance of the beams kept increasing, where larger portions of the steel cross-section underwent yielding. Transverse cracks started to appear at the bottom side of the concrete slabs after yielding of the steel section, as shown in Fig. 13(a). The width of the transverse cracks kept increasing until the end of the test. Longitudinal cracks were observed for the same beams at the upper side of the concrete slabs just before failure occurs. The longitudinal cracks were initiated at the upper side of the concrete slab due to the absence of upper reinforcement, as shown in Fig. 13(b). It should also be noted that the development of the longitudinal cracks was always associated with an increase in the slip values at the interface between the concrete slab and the steel beam. These longitudinal cracks were developed due to the concentrated force applied by the shear connectors which leads to transverse tension in the concrete slab. The longitudinal crack width at the top of the concrete slab kept increasing and propagating till the end of the test. On the other hand, the compressive strains at the upper fibers of the concrete slab did not reach

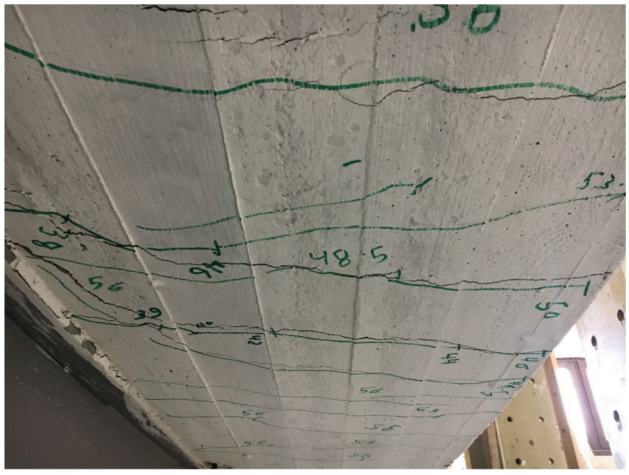

(a) Transverse cracks at the lower surface of the concrete slab

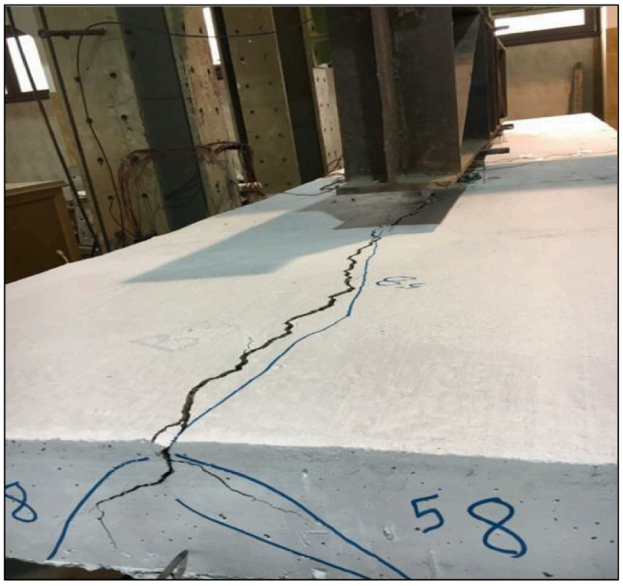

(b) Longitudinal cracks in beams without uppersteel rebars

Fig. 13. Different crack patterns of tested beams.

the crushing strain of concrete and hence no sign of compressive failure was observed. It should be noted that beams B1 and B2 failed just before the concrete slabs reach the crushing strain.

Group 2 includes Beams B5 and B6 with upper reinforcement steel mesh in the concrete slab (higher reinforcement ratios), which followed the same failure mechanism described for the previous group without experiencing any longitudinal cracks. This is attributed to the presence of the upper steel reinforcement mesh. In particular, the transverse steel rebars prevented the longitudinal cracking of the concrete slab at the top surface. It should also be noted that this group of beams achieved the highest slip values at the interface between steel and concrete (1.97 mm and 1.91 mm), respectively Moreover, the high reinforcement ratios of the concrete slabs of beams B5 and B6 allowed for full utilization of the steel beam, where almost the entire steel cross-sections reached their yielding strains, as shown in Fig. 10.

Group 3 includes beams B9 and B10, which started with underside concrete cracking before the initiation of yielding of the steel cross-section. The tensile strain at the underside of the concrete slab exceeded the allowable tensile strain of concrete in tension. This is attributed to the small size of the steel section compared to the concrete slab, which allocated the neutral axis inside the concrete slab and read tensile strains

at the underside of the concrete slab early from the beginning of the test. After that, the loading resistance of the beams kept increasing, where larger portions of the steel cross-section underwent yielding.

5. Conclusions

The findings of this study highlight the factors affecting the slip and strain distribution along the concrete slab of composite beams. The following conclusions can be drawn :

It is found that when the used shear connectors are not capable of achieving the full composite actions the channel shear connectors are usually stiffer than the angle shear connectors in resisting the slip of concrete slab by about 30% within the elastic range. The effect of the shear connector type on the slip values diminishes when the composite beams are designed with full-composite action.

The effect of using channels as shear connectors on the ultimate strength is more pronounced for beams with full-composite action. The ultimate load capacity of composite beam with channel connectors achieving full composite action (P/S = 1.14) is higher than the counterpart composite beam with angle connectors by 14%.

The strain incompatibility at the interface between steel and concrete in partially composite beams is more pronounced with angle connectors when compared to channel connectors.

Beams with angle connectors experience earlier initiation of tension zones at the bottom of the concrete slab than beams with channel connectors.

It is found that the upper steel reinforcement enhances the stress distribution along the concrete slab. Uniform stress distribution along the concrete slab is observed at the ultimate stage. It is found that by increasing the reinforcement ratio of the concrete slab from 0.18% (B3) to 0.46% (B5), for beams provided with channel shear connectors, the flexural strength of the composite beams was increased by 7.45% and the deflection values were dropped by 23%. On the other hand, the effect of reinforcement mesh becomes less effective with thinner concrete slabs.

Using transverse steel reinforcement in the concrete slab prevented any longitudinal cracks at the top surface of the concrete slab and allowed for full plastification of the steel cross-sections.

Poisson's ratio of the concrete slab is found constant throughout the test with a value of 0.16 and dramatically increases before failure occurs.

CRediT authorship contribution statement

Ahmed Kamar: Investigation, Funding acquisition, Writing - original draft. **Mahmoud Lasheen:** Conceptualization, Methodology, Resources, Software, Writing - original draft, Data curation, Visualization, Investigation, Supervision, Writing - review & editing. **Amr Shaat:** Conceptualization, Methodology, Software, Writing - original draft, Investigation, Visualization, Supervision, Writing - review & editing. **Amr Zaher:** Supervision. **Ayman Khalil:** Supervision.

Declaration of Competing Interest

The authors declare that they have no known competing financial interests or personal relationships that could have appeared to influence the work reported in this paper.

References

[1] Lam D, El-Lobody E. Behaviour of Headed Stud Shear Connectors in Composite Beam. J Struct Eng 2005;131(1):96–107.

[2] Classen M, Hegger J. Shear-slip behaviour and ductility of composite dowel connectors with pry-out failure. Eng Struct 2017;150:428–37.

[3] Classen M, Herbrand M, Adam V, Kueres D, Sarac M. Puzzle-shaped rib shear connectors subjected to combined shear and tension. J Constr Steel Res 2018;145:232–43.

[4] Lorenc, W., Kubica, E. and Kożuch, M. Testing procedures in evaluation of resistance of innovative shear connection with composite dowels. Archives of Civil and Mechanical Engineering. Vol. 10, issues 3, pp. 51-63.

[5] Nie J, Cai CS. Steel-Concrete composite beams considering shear slip effects. J. Struct. Eng. ASCE 2003;129(4):495–506.

[6] Ros S, Shima H. A New Beam Type Test Method for Load-Slip Relationship of L-Shape Shear Connector, The 8th Symposium on Research and Application of Hybrid and Composite Structures. Japan Society of Civil Engineers 2009:1–8.

[7] Kiyomiya O, Yokota H, Suzuki M, Chiba T. Strength Properties of Shear Connectors by Shape Steel. Transactions of the Japan Concrete Institute 1986.

[8] Shariati M, Ramli Sulong NH, Suhatril M, Shariati A, Arabnejad Khanouki MM, Sinaei H. Behaviour of C-shaped angle shear connectors under monotonic and fully reversed cyclic loading: an experimental study. Mater Des 2012;41:67–73.

[9] Shariati A, Shariati M, Ramli Sulong NH, Suhatril M, Arabnejad Khanouki MM, Mahoutian M. Experimental assessment of angle shear connectors under monotonic and fully reversed cyclic loading in high strength concrete. Constr Build Mater 2014;52:276–83.

[10] Shariati M, Shariati A, Ramli Sulong NH, Suhatril M, Arabnejad Khanouki MM. Fatigue energy dissipation and failure analysis of angle shear connectors embedded in high strength concrete. Eng Fail Anal 2014;41:124–34.

[11] Classen M. Limitations on the use of partial shear connection in composite beams with steel T-sections and uniformly spaced rib shear connectors. J Constr Steel Res 2018;142:99–112.

[12] Classen, M., Stark, A., and Hegger, J. (2017). Steel-HSC composite beams with partial shear connection and miniaturized limited-slip-capacity connectors. Vol. 11, issue 1, pp. 94-103.

[13] Classen M, Herbrand M. Minimum partial shear connection of composite beams with small scaled shear connectors - Derivation of the minimum degree of partial shear connection by systematic use of nonlinear Finite Element Analysis (FEA). Bauingenieur 2016;91:140–51.

[14] Pfenning S, Brunkhorst S, Mensinger M, Zehfuss J. Minimum degree of shear connection of composite beams in fire. STAHLBAU 2019;88(3):234–46.

[15] Chiewanichakorn M, Aref A, Chen S, Ahn I. Effective flange width definition for steel– concrete composite bridge Girder. J. Struct. Eng., ASCE 2004;130(12):2016–31.

[16] Lasheen M, Shaat A, Khalil A. Behaviour of lightweight concrete slabs acting compositely with steel I-sections. Constr Build Mater 2016;124:967–81.

[17] Sedlacek G, Bild SA. Simplified method for the determination of the effective width due to shear lag effects. J Constr Steel Res 1993;24:15582.

[18] Dezi L, Gara F, Leoni G, Tarantino AM. Time-dependent analysis of shear-lag effect in composite beams. J Eng Mech 2001;127(1):71–9.

[19] Amadio C, Fedrigo C, Fragiacomo M, Macorini L. Experimental evaluation of effective width in steel–concrete composite beams. J Constr Steel Res 2004;60(2):199–220.

[20] Lasheen M, Shaat A, Khalil A. Numerical evaluation for the effective slab width of steel-concrete composite beams. J Constr Steel Res 2018;148:124–37.

[21] American Institute of Steel Construction, ANSI/AISC-360-15.Specifications for Structural Steel Buildings, Chicago, Illinois.

[22] Canadian Standards Association, CAN/CSA-S16-14, Limit states design of steel structures, Mississauga, Ontario.

[23] Eurocode, Design of Composite Steel and Concrete Structures. Part 1. 1: General Rules and Rules for Buildings, 2004.

[24] Classen M, Hegger J. Assessing the pry-out resistance of open rib shear connectors in cracked concrete – Engineering model with aggregate interlock. Eng Struct 2017;148:254–62.